Subpolar High Anomaly Preconditioning Precipitation over South America

SILVINA A. SOLMAN

Centro de Investigaciones del Mar y la Atmósfera, CONICET-UBA, Buenos Aires, Argentina

ISIDORO ORLANSKI

Atmospheric and Oceanic Sciences Program, Princeton University, Princeton, New Jersey

(Manuscript received 4 September 2009, in final form 29 December 2009)

ABSTRACT

The mechanisms associated with the intraseasonal variability of precipitation over South America during the spring season are investigated with emphasis on the influence of a quasi-stationary anomalous circulation over the southeastern South Pacific Ocean (SEP). A spectral analysis performed to the bandpass-filtered time series of daily precipitation anomalies for the La Plata Basin (LPB) and the South Atlantic convergence zone (SACZ) regions revealed several statistically relevant peaks corresponding to periods of roughly 23 days and 14–16 days—the lower (higher) frequency peaks more prevalent for the SACZ (LPB). The large-scale circulation patterns preconditioning precipitation variability over both regions were explored by means of a regression analysis performed on the daily 500-hPa geopotential anomaly field provided by the NCEP–NCAR reanalysis dataset. The most prominent feature of the regression fields is the presence of a quasi-stationary anomalous anticyclonic (cyclonic) circulation over the southeastern South Pacific Ocean associated with positive rainfall anomalies over the LPB (SACZ) and, emanating from that high (low), an external Rossby wave propagating northeastward toward the South American continent. The synoptic-scale activity, quantified in terms of a frontal activity index, showed a strong influence on precipitation over the LPB and to a lesser extent over the SACZ. Moreover, the frontal activity is actually modulated by the anomalous high circulation over the SEP region. The behavior of this anomalous circulation may be supported by a positive feedback mechanism that can enhance the response of the high anomaly itself, which in turns reinforces the Rossby wave train propagating toward the South American continent.

1. Introduction

The warm-season precipitation in subtropical South America is characterized mainly by an organized branch of convective activity extending from the Amazon toward the southeast into the South Atlantic Ocean, referred to as the South Atlantic convergence zone (SACZ), and a secondary maximum of rainfall extending over southeastern South America, comprising northeastern Argentina, Uruguay, southern Paraguay, and southern Brazil, referred to as the La Plata Basin region (hereafter LPB). Several studies have focused on characterizing the intraseasonal variability of summer precipitation over South America and several explanations to the triggering mechanisms have been proposed. Using outgoing longwave radiation (OLR) as a measure of convection and, hence, as a proxy of precipitation, Nogués-Paegle and Mo (1997) showed that during the austral summer season [December–February (DJF)] the leading mode of intraseasonal variability of rainfall has a dipole structure with enhanced (reduced) rainfall over the SACZ accompanied by decreased (increased) rainfall over the LPB—referred to as the South American see-saw pattern. They also showed that this behavior is related to the strength and direction of the low-level circulation. When the low-level jet located east of the Andes has a strong southward component, the moisture flux from the Amazon region converges over the subtropical plains and precipitation over the LPB (SACZ) is enhanced (weakened). Conversely, when the low-level circulation acquires a zonal direction at about 20°S, the low-level jet weakens and the moisture flux converges over the SACZ region, enhancing precipitation over that area. Nogués-Paegle and Mo (1997)

Corresponding author address: Silvina A. Solman, CIMA (CONICET-UBA), Ciudad Universitaria, Pabellón II-2do. Piso (C1428EGA), Buenos Aires, Argentina.
E-mail: solman@cima.fcen.uba.ar

DOI: 10.1175/2009JAS3309.1

related this behavior to a zonal shift of the South Atlantic subtropical high.

To identify the characteristic time scales leading the intraseasonal variability of the dipole pattern, Nogués-Paegle et al. (2000) analyzed the dominant periods of variability of summer convection by means of singular spectrum analysis. They showed that the intraseasonal modulation of convection over the SACZ is dominated by two modes of different time scales. Both oscillatory modes with periods of 40–60 days and 22–28 days, respectively, influence convection variability over the SACZ but the faster mode leads the variability over the subtropical plains. They suggest that the submonthly mode is forced by a Rossby wave train propagating eastward across the central Pacific at 60°S and then curving toward the northeast over South America. Liebmann et al. (1999) also showed that submonthly variations of convection over the SACZ are influenced by a Rossby wave pattern, originating within the midlatitudes westerly belt in the Pacific Ocean, that propagates northeastward, influenced by the Andes and the Antarctic Plateau (Ambrizzi and Hoskins 1997). They also suggest that the preferred path of equatorward Rossby wave propagation over South America is related to the large-scale basic state generated by large-scale sources and sinks of diabatic heating, such as Amazon convection. Grimm and Silva Dias (1995) found that divergence over the region of the South Pacific convergence zone exerts an influence on convection over the SACZ through Rossby wave propagation. Each of the aforementioned studies suggests that the intraseasonal variability of the warm-season rainfall over South America is influenced by mechanisms originating in the tropics.

More recently, Liebmann et al. (2004) suggested that the phase of the Rossby wave train determines whether rainfall will be enhanced over the subtropical plains of South America or over the SACZ, contributing to the out-of-phase relationship of rainfall over both regions. However, they did not explore the triggering mechanism for this wave train.

It has also been recognized that synoptic-scale activity plays an important role in triggering rainfall events over the LPB and SACZ (Vera et al. 2002; Garreaud and Wallace 1998; Liebmann et al. 1999). Cunningham and Cavalcanti (2006) have recently shown that the high-frequency systems associated with frontal activity in the presence of the tropical/extratropical mode, such as the Pacific–South America (PSA) mode, could trigger convective pulses over the SACZ. They suggest that an adequate phasing between the patterns of low-frequency and high-frequency circulation variability is needed to create conditions for more permanent convective episodes over the SACZ.

In this work we will demonstrate that the presence of an anomalous high circulation located over the southeastern Pacific Ocean, with characteristic time scales within the intraseasonal range, preconditions precipitation over South America mainly through two independent mechanisms. In the first place, this anomalous high is the source of an external Rossby wave that propagates toward South America, which establishes an anticyclonic circulation over the northeast LPB. The anomalous anticyclonic circulation over the northeast LPB enhances moisture transport toward the LPB region and consequently enhances rainfall over that area. This mechanism controls rainfall variability on submonthly time scales. On the other hand, we will explore the large-scale circulation patterns that precondition the preferred paths of the high-frequency systems. Our hypothesis is that the frontal systems that trigger rainfall events, mainly over the LPB, are strongly affected by the anomalous high circulation located over the southeastern South Pacific, which acts as a blocking anticyclone affecting the path of the frontal systems propagating toward South America. We suggest that the anomalous high forces the frontal systems to acquire a northward propagation, forcing them to penetrate into subtropical latitudes over the South American continent instead of propagating eastward.

The anomalous high preconditioning precipitation over South America has been referred to in previous studies of the impact of blocking anticyclones on climate (Mendes et al. 2008; Kayano 1999); moreover, the presence of this anomalous circulation over the southeastern Pacific has been implicitly considered as part of a larger-scale pattern of circulation variability. The mechanisms explaining why this anomalous high is maintained are outside of the scope of the present paper and will be elucidated elsewhere.

Most of the previous studies have focused on understanding the forcing mechanisms of intraseasonal variability of summer-season rainfall over South America, when tropical convection over the Amazon Basin and over the SACZ region are the most distinctive features. Consequently, considerable attention has been given to the intraseasonal variability over the SACZ (Carvalho et al. 2004). The onset of the rainy season over most of South America starts in austral spring and rainfall peaks during austral summer. However, the annual cycle of rainfall over the LPB region is different from that of the SACZ. Figure 1a shows the monthly climatology of rainfall over both regions. In the LPB region maximum precipitation is during late summer to early fall (February and April) and in late spring (November) rather than during summer, as for SACZ. We are now interested in the austral spring season, October–December (OND), because we are more interested in understanding the intraseasonal variability of precipitation over the LPB region.

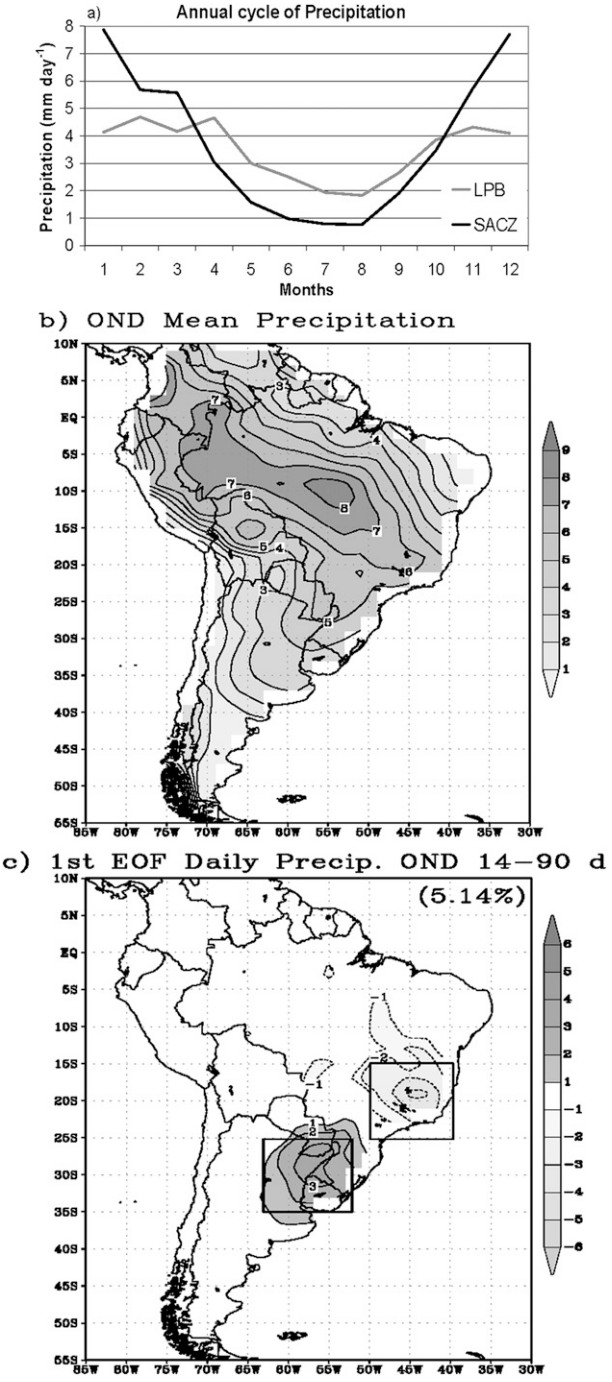

FIG. 1. (a) Annual cycle of precipitation over the SACZ (black line) and LPB (gray line). (b) Climatological OND precipitation for the period 1979–99, contours every 1 mm day^{-1} and values greater than 2 mm day^{-1} shaded. (c) Precipitation anomaly field regressed upon the principal component time series corresponding to the first EOF pattern of the OND daily precipitation filtered on the 14–90-day band, computed for the period 1979–99. The variance explained is indicated as a percentage. Contour interval is 1 mm day^{-1}. The two boxes define the areas where the precipitation was averaged to define the SACZ and LPB precipitation time series, respectively.

Moreover, the austral spring season is interesting because it is the time of the year when the interaction between convective triggering and synoptic wave forcing is a relevant mechanism associated with rain events. Consequently, one of the main objectives of this work is to characterize the intraseasonal variability of precipitation over the LPB region during the spring season.

Figure 1b shows the climatology of rainfall during OND over South America for the period 1979–99. Two regions are of particular interest: a band extending in the northwest to southeast direction where precipitation is maximal, referred to as the SACZ, and a branch of large precipitation extending across the LPB region. The main pattern of intraseasonal variability of rainfall during the austral spring season (Fig. 1c) shows a dipole pattern structure, similar to the pattern derived by Nogués-Paegle and Mo (1997) using OLR anomalies for DJF. We will concentrate on the time evolution of the precipitation anomalies over the SACZ and LPB regions, indicated by the boxes in Fig. 1c.

The paper is organized as follows. In section 2 the datasets and methodology are described. Section 3 discusses the time scales of variability of the daily precipitation time series over LPB and SACZ and the circulation patterns associated with rainfall anomalies over both regions. Section 4 is devoted to exploring the time scales of variability of the circulation patterns in the Southern Hemisphere and the connection with the quasi-stationary anomalous high located over the southeastern South Pacific Ocean. A discussion of the results and conclusions are presented in section 5. Finally, an appendix with results obtained with a numerical model showing how external Rossby waves can be excited by the anomalous high over the periphery of the polar cap, as demonstrated by Orlanski and Solman (2010, hereafter OS10) is also included.

2. Data and methodology

Daily precipitation data on a 2° global grid for the period from 1979 to 1999 was used to describe the precipitation anomalies over South America. This dataset was derived based on global station observations from the Climate Prediction Center (CPC). The CPC ''summary of day'' data, derived from 3-hourly synoptic reports from the stations contributing to the Daily World Meteorological Data Network of the World Meteorological Organization, was used to compute areal precipitation over land. More details on this database can be found in Nijssen et al. (2001). We also used daily mean OLR data from the NOAA interpolated OLR database (Liebmann and Smith 1996) for the period 1979–99 on a 2.5° grid. OLR data was used to assess to what extent

it is able to reproduce the same features of the intraseasonal variability for OND over South America as precipitation data. The circulation fields used in this study come from the National Centers for Environmental Prediction (NCEP)–National Center for Atmospheric Research (NCAR) reanalysis on a 2.5° grid for the period 1979–99 (Kalnay et al. 1996). We have used mainly daily 500-hPa geopotential fields, taking only one analysis per day, at 1200 UTC. However, for some analyses we have also used other variables from the NCEP–NCAR database, such as 850-hPa temperature and horizontal winds.

The period from 1 October to 31 December was selected as representative of the austral spring season. For all variables used, daily anomalies were defined as the difference between the daily value and monthly climatological mean for the period 1979–99, removing most of the seasonal cycle. To focus our attention on the intraseasonal band the daily datasets were filtered using a bandpass Lanczos filter with 501 daily weights (Duchon 1979). Daily anomalies were filtered to retain the variability within 4 to 100 days. This filtering allows retaining the main frequencies expected to dominate the intraseasonal and synoptic-scale variability of precipitation.

According to the spatial distribution of the first mode of intraseasonal variability of the precipitation field (Fig. 1c), after an empirical orthogonal function analysis performed on the filtered precipitation anomalies for OND over South America (retaining periods from 14 to 90 days), two regions representing the main centers of action of the see-saw pattern were identified. Areal averages over these two boxes were calculated to define the SACZ and LPB precipitation time series, respectively. For the SACZ region we performed an area average from 25° to 15°S, 50° to 40°W. For the LPB region, the box was defined from 35° to 25°S, 63° to 53°W. The boxes are indicated in Fig. 1b.

The main analysis tool used to examine the relationship between circulation patterns and precipitation over SACZ and LPB is based on regression analysis. This technique has been used in various studies and its advantage is that the regression coefficients carry the units of the regressed variable and may be interpreted as the amplitude of the anomalies at each grid point that are observed in association with an anomaly of the reference variable with an amplitude of one standard deviation. Moreover, the lagged regression maps allow one to infer the temporal evolution of the relationship explored. Lagged regression maps were computed using the time series of daily precipitation anomalies averaged over the SACZ and LPB, respectively, and the daily anomalies of the 500-hPa geopotential fields at global scale. The statistical significance of the corresponding correlation coefficients, that is, the regression coefficients normalized by the standard deviation of the 500-hPa geopotential anomaly field, has been assessed using a Fisher test. The number of degrees of freedom was adjusted based on the lag-1 autocorrelation coefficient of the time series built as the product of the anomalies considered in the correlation (Wilks 1995).

3. Results

a. Variability of the daily precipitation time series over the SACZ and LPB

To discuss the time scales of variability of OND precipitation, we have performed a spectral analysis on the filtered time series of precipitation anomalies for both the SACZ and LPB, as in Liebmann et al. (1999). Two months before and after the target season were included in the analysis so as to construct a 212-day time series for each year. However, we have applied a 60-day taper to each end of the series (Bloomfield 1976) to emphasize only the OND months. The spectral analysis was performed for each of the 212-day time series and averaged over the 21 years of record.

Still, to be certain about the spectral analysis for precipitation we have taken time series over the same areas using OLR anomalies and performed the same analysis. The spectra for both precipitation and OLR anomalies over the SACZ and LPB for OND are shown in Fig. 2. The dashed curves in Fig. 2 show the red-noise spectrum based on the lag-1 autocorrelation for the SACZ series. As expected, the two independent spectra are consistent. Although some of the spectral peaks corresponding to the lower frequencies lie slightly below the red-noise spectrum, we consider them to be still robust because they result from an average spectrum constructed as the mean of the 21 individual spectra. For the SACZ time series a robust peak is found confined within the low-frequency band, from 26 to 23 days, and several statistically significant secondary peaks at higher frequencies. The amplitude of the main peak is larger for the longer periods, suggesting that the intraseasonal variability prevails compared with synoptic-scale variability. When we look to the LPB, the spectrum is flatter. The relative amplitude of the higher-frequency peaks becomes larger compared with the SACZ, confirming that the variability of precipitation over the LPB region is dominated by both a submonthly mode on the intraseasonal time scale and the synoptic-scale variability, in agreement with Liebmann et al. (1999) and Nogués-Paegle et al. (2000). Since part of the synoptic-scale variability was removed when filtering the anomalies to retain the 4–100-day period, we also performed the spectral analysis using a bandpass filter retaining periods from 2.5 to 100 days. The results were found to be similar in the context of what is

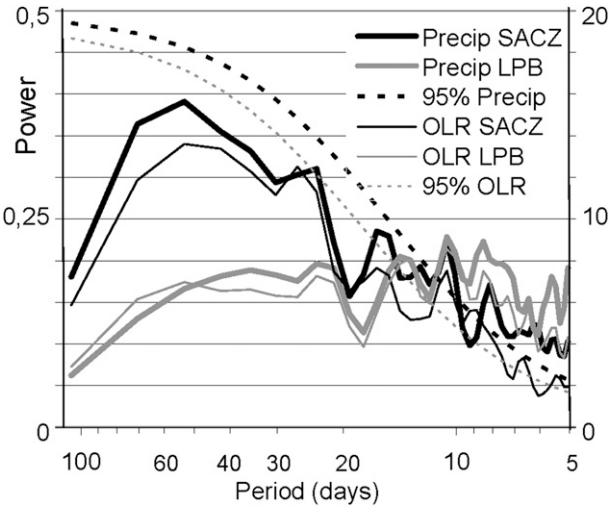

FIG. 2. Average power spectra of OND precipitation (thick lines) and OLR (thin lines) computed for the corresponding time series constructed for the SACZ (black lines) and LPB (gray lines). Also shown is the red noise spectrum (dashed curve) corresponding to the SACZ series.

discussed concerning the behavior of the SACZ and LPB time series for both precipitation and OLR. As expected, the percentage of variance within the higher frequencies (less than 15 days) increased up to 48% (27%) of the total variance for the precipitation time series over the LPB (SACZ) as compared with 42% (24%) obtained with the former filter, whereas the percentage of variance within the lower frequencies is close to 50% (71%).

b. Circulation patterns associated with rainfall anomalies over the SACZ and the LPB regions

To examine the circulation anomalies controlling rainfall variability over the SACZ and LPB we performed a regression analysis based on the daily anomalous precipitation time series, averaged over both regions, and the 500-hPa geopotential anomalies on a global grid, shown in Fig. 3. The zonal mean has been subtracted from the geopotential anomaly field so as to better capture the wave structure of the pattern. The regression for LPB (Fig. 3a) shows that, associated with positive rainfall anomalies over the LPB region, there is a large positive height anomaly over the Bellingshausen Sea region in the southeastern South Pacific and, emanating from that high, a trend of external Rossby waves downstream of the anomalous high. The pattern over South America is very similar to what has been reported in the literature (Liebmann et al. 2004). Inspection of the regression at the 850-hPa level (not shown) revealed that the wave train pattern has an equivalent barotropic structure. The positive rainfall anomalies over the LPB are associated with an anomalous anticyclonic circulation over the subtropical Atlantic Ocean, which reinforces the subtropical anticyclone and a cyclonic circulation over central South America. These circulation anomalies reinforce the northwesterly flow and enhance the moisture transport to the LPB region, in agreement with previous studies (Nogués-Paegle and Mo 1997; Liebmann et al. 2004; Díaz and Aceituno 2003). The amplitude of the regression is particularly large in the branch extending from the high in the southeastern Pacific toward South America, which may be due to the method of regression that shows larger amplitudes in the neighborhood of the location where the time series is defined, compared with other regions.

The regression for the SACZ (Fig. 3b) shows that in the region close to southwestern South America, the pattern is exactly reversed compared with the regression for the LPB. Specifically, over the Bellingshausen Sea there is a negative height anomaly associated with positive rainfall anomalies over the SACZ, and the circulation over South America is opposite of what is shown for the regression with precipitation time series for the LPB. However, the hemispheric pattern of the regression seems to be more wavy, with wavenumber 3 for the SACZ and more significance farther from the SACZ area, whereas for the LPB the wave pattern is not clearly evident. The regressions were also performed using streamfunctions (not shown), and the results found were similar to those shown in Fig. 3.

The regression maps displayed in Fig. 3 show a wave pattern propagating over the midlatitudes throughout the Pacific Ocean that resembles the well-known Pacific–South American mode (PSA2) (Ghil and Mo 1991), one of the leading modes of variability of the atmospheric circulation on the intraseasonal time scale, whose development has been associated with tropical convection (Mo and Higgins 1998). However, it is clear from Fig. 3 that the amplitude of the circulation anomalies becomes larger over the Bellingshausen Sea and the Rossby wave pattern seems to emanate from that region. Conversely, the regression with precipitation for the SACZ (Fig. 3b) suggests a wave train that may originate somewhere over the southern Indian Ocean. The Indian Ocean dipole (Chan et al. 2008), which has its largest amplitude during the austral spring season, may also play a role in forcing a Rossby wave pattern. Moreover, these authors have shown that on interannual time scales a significant teleconnection pattern is found between the Indian Ocean dipole and rainfall variability over the LPB and central Brazil, which manifests also as a dipole pattern in the regional rainfall anomalies.

To explore the time evolution of this circulation pattern, we perfomed time-lagged regression analysis of the 500-hPa geopotential anomaly field from 10 days prior to 10 days after the precipitation event over the LPB,

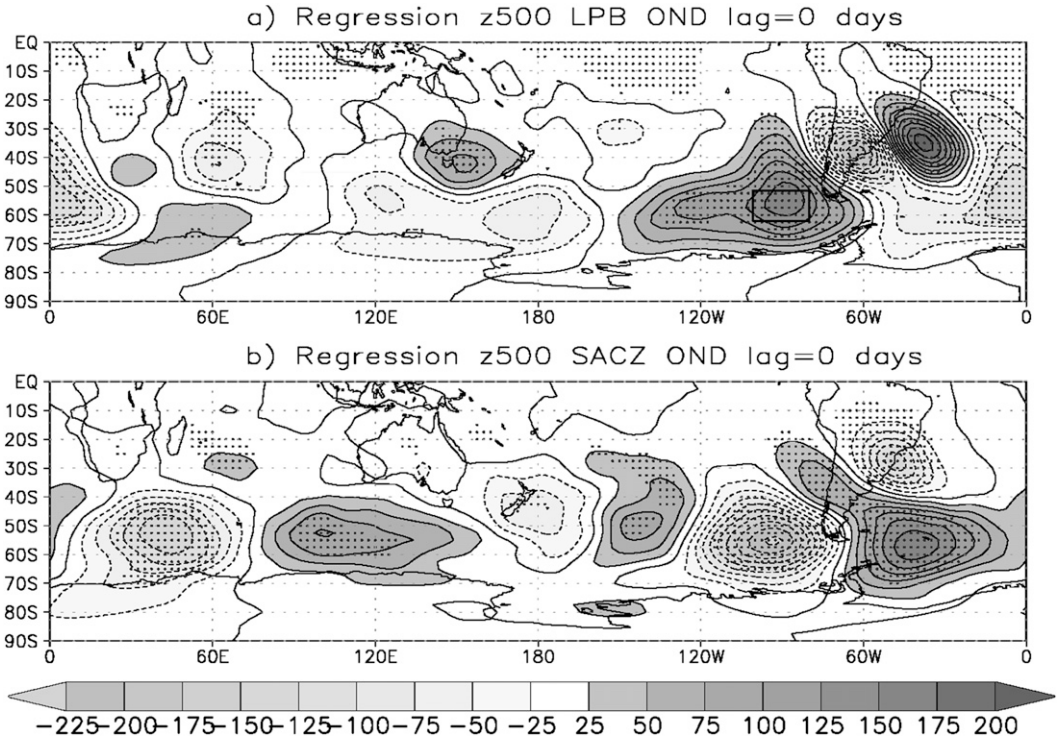

FIG. 3. Regression of the 500-hPa geopotential field with the precipitation time series corresponding to (a) LPB and (b) SACZ. Contours are drawn every 25 $m^2\ s^{-2}$. Light (dark) shading and dashed (solid) lines correspond to negative (positive) values. Stippled areas indicate where the correlation between the two variables is significant at the 95% confidence level, based on the *F* statistic, taking into account adjusted degrees of freedom based on the lag-1 autocorrelation. The box in (a) defines the SEP area, where the anomalies of 500-hPa heights were averaged to define the SEPz time series.

shown in Fig. 4. Negative (positive) lags account for the circulation anomalous field before (after) the occurrence of anomalous precipitation over the target region. The regression was done using unfiltered data. However, we also examined the lagged regressions after bandpass filtering both variables and found similar results. It is evident from Fig. 4 that on a scale of 20 days the pattern changes drastically. We note that the high–low system over the middle of South America is very weak or nonexistent 10 days prior and 10 days after the rain event; also, the most remarkable feature, the anomalous high, appears to be close to the Ross Sea at lag −10 days, moves to the Bellingshausen area at lag 0, and repeats the same pattern at lag +10 days. We have also performed a time-lagged regression analysis using the 500-hPa height anomaly fields with the anomalous precipitation time series over the SACZ (not shown) and found that the patterns are reversed compared with those shown in Fig. 4.

It seems clear from Fig. 4 that the regression of the 500-hPa geopotential anomaly field with precipitation over the LPB shows a clear pattern only at lag 0 rather than at −10 and 10 days. Moreover, the largest response seems to be related to the effect of a pattern that originates or is enhanced over the southeastern Pacific, producing a wave pattern that spreads into the South American region. To better understand this pattern we centered our attention on a time series over the anomalous high in the southeastern South Pacific. This time series is defined as the area average of the daily anomalies of the 500-hPa geopotential height in the box shown in Fig. 3a. This time series is referred to as the SEPz index.

Figure 5 shows the mean spectrum of the SEPz time series, computed in the same way as those spectra shown in Fig. 2. It is clear that three peaks emerge from the spectrum: one centered on 50 days, another on 23 days, and the third on about 16 days. The prominent peaks in the spectrum of SEPz closly correspond with those found for LPB and SACZ precipitation and OLR time series. This behavior suggests that the intraseasonal variability of precipitation over the LPB and SACZ is strongly related to the variability of the anomalous circulation in the southeastern Pacific. Moreover, the main periods of oscillation found for the SEPz time series are also consistent with the dominant periods of the corresponding

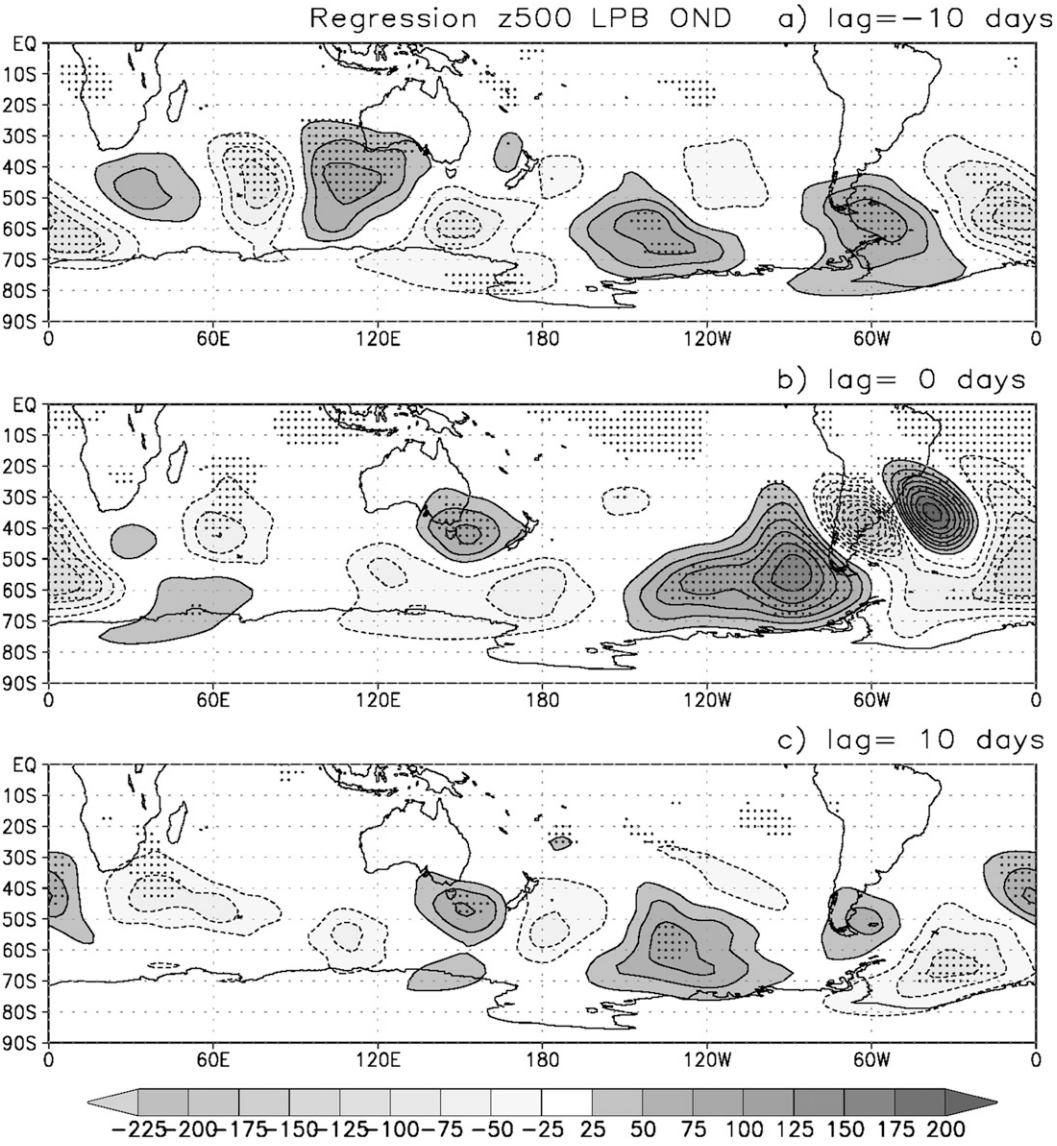

FIG. 4. Lagged regression of the 500-hPa geopotential field with the precipitation time series corresponding to LPB for lags (a) −10, (b) 0, and (c) +10. Contours are drawn every 25 m^2 s^{-2}, zero contours omitted. Light (dark) shading and dashed (solid) lines correspond to negative (positive) values. Stippled areas indicate where the correlation between the two variables is significant at the 95% confidence level.

time series of the PSA2 pattern reported by Mo and Higgins (1998).

In fact, not only are the dominant periods of the SEPz time series similar to those found for the PSA2 mode, but also the regression of the 500-hPa geopotential anomaly field with the SEPz time series, shown in Fig. 6, looks like the PSA2 pattern reported in Mo and Higgins (1998). We calculated the regression maps using the unfiltered data and also using different bandpass filters retaining the periods corresponding to the three main peaks shown in Fig. 5. The results are depicted in Fig. 6. The regression maps look similar to the PSA2 pattern for both the unfiltered and filtered data. The only difference among the panels in Fig. 6 is the amplitude and spatial scale, with the regressions computed for the lower (higher) frequencies characterized by a larger (smaller) spatial scale. The pattern of the arc bending northward over South America, shown in the regression computed with the nonfiltered data, seems to appear in the higher-frequency regression field (periods 14–17 days). Conversely, the regressions retaining the lower frequencies seem to show a more zonal structure.

To explore to what extent the anomalous high over the southeastern Pacific Ocean might control the precipitation

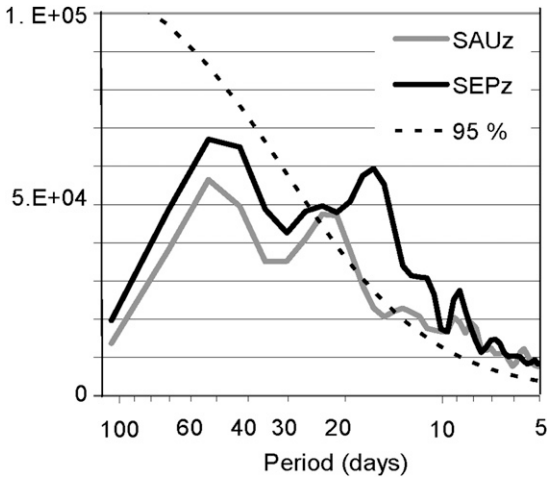

FIG. 5. As in Fig. 2 but for the SEPz and SAUz time series.

variability over South America, we calculated the regression of the daily precipitation anomaly field with the SEPz time series. This is shown in Fig. 7. Over LPB (SACZ), positive (negative) precipitation anomalies are related to positive height anomalies over the SEP box. Figure 7 shows a pattern that resembles the first mode of variability of the daily precipitation field depicted in Fig. 1c. However, the regression seems to be stronger for the LPB region, compared with SACZ. We also calculated the regression after bandpass filtering both variables so as to retain the intraseasonal band (with periods of 14–90 days) and the results found were similar (not shown). These results are also in agreement with Kayano (1999) and Mendes et al. (2008), who assessed the climate impact of blocking episodes over continental areas of South America and found that blocking anticyclones that are frequent during the spring season in the southeastern Pacific Ocean are related to wetter than normal conditions over southeastern South America.

The daily precipitation dataset used in this study covers only continental areas. To have a broader picture of the relationship between the anomalous high over the SEP region and the precipitation anomaly field, we calculated the regression of the daily OLR anomaly field with the SEPz time series, shown in Fig. 8a. First, the regression with OLR tends to verify a pattern similar to that for the precipitation data over South America. To be noticed in this regression is the large band that extends over the subtropical Pacific and the southeastern Atlantic—referred to later on as to the negative OLR anomaly. Note also a small negative OLR anomaly over the periphery of Antarctica centered at 120°W, which is actually located to the southwest of the anomalous high. Although OLR is a reliable measure of convective activity mainly for tropical and subtropical areas and is less reliable over high latitudes, particularly over snow-covered areas, the negative anomaly along the coastline of Antarctica is physically consistent, as will be shown later.

c. *High-frequency circulation anomalies associated with rainfall anomalies over the SACZ and LPB regions*

The displacement of frontal systems from high latitudes toward southeastern South America is found to act as one of the triggering mechanisms that organize convection over the LPB and SACZ (Salio et al. 2007; Cunningham and Cavalcanti 2006). The frontal activity, particularly active during the spring season, might trigger severe storms in unstable atmospheric environments, such as prefrontal squall lines and mesoscale convective systems, which are particularly frequent over southeastern South America during the spring season (Salio et al. 2007; Velasco and Fritsch 1987). Siqueira and Machado (2004) found that the penetration of cold fronts into subtropical South America influences the variability of convection over the tropics and subtropics on synoptic time scales.

To investigate the influence of synoptic-scale activity on precipitation variability over the LPB and SACZ, we explored the relationship between anomalous rainfall and frontal activity. The frontal activity has been defined in terms of an index, referred to as the Front Activity index (FI), which has been calculated as the product between the absolute value of the 850-hPa temperature gradient and the absolute value of the relative vorticity (ξ):

$$\mathrm{FI} = \left|\nabla T_{850\mathrm{hPa}}\right| \times \left|\xi_{850\mathrm{hPa}}\right|.$$

This index has been derived at every grid point using 6-hourly data (850-hPa temperature and winds) from the NCEP–NCAR reanalysis data and the daily mean values were computed. Cold fronts are associated with strong negative relative vorticity in the Southern Hemisphere and strong horizontal temperature gradients; hence, large values of the absolute values of both quantities and, consequently, large values of the FI are expected to be related, particularly with the passage of cold fronts. The FI is a daily two-dimensional field covering the period from 1979 to 1999. Note that the sign of relative vorticity is opposite in the SH to that in the Northern Hemisphere.

The frontal activity might be influenced by the presence of the anomalous high over the southeastern South Pacific Ocean, which may influence the trajectory of the synoptic systems and consequently influence precipitation variability. To explore this possibility we calculated the regression of the FI with the SEPz time series, shown in Fig. 8b. It is interesting to note a maximum of frontal

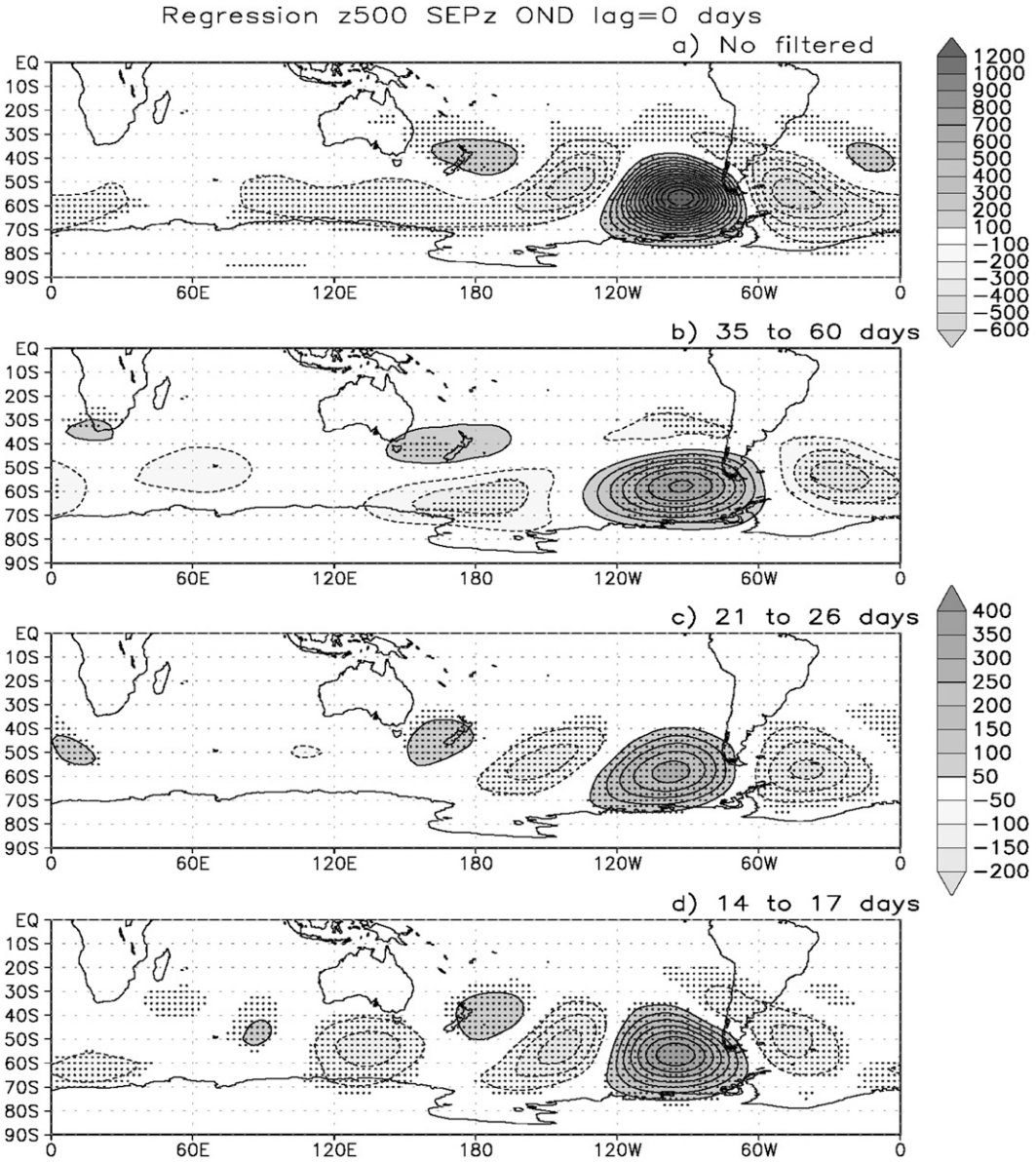

FIG. 6. Regression of the 500-hPa geopotential field with the SEPz time series for (a) unfiltered anomalies and for filtered anomalies retaining periods (b) 35–60 days, (c) 21–26 days, and (d) 14–17 days. Light (dark) shading and dashed (solid) lines correspond to negative (positive) values. Contours are drawn every 100 m^2 s^{-2}, zero contours omitted. Stippled areas indicate where the correlation between the two variables is significant at the 95% confidence level.

activity over the Southern Hemisphere related to a positive/negative anomaly over the southeastern Pacific Ocean corresponding to the storm track region, as expected (Hoskins and Hodges 2005). However, there are three areas worth mentioning. There is a maximum on the periphery of Antarctica, from the Ross Sea to the Palmer Peninsula, and an extended maximum over subtropical South America and the South Atlantic region. The maximum over subtropical South America correlates well with the negative OLR anomaly shown in Fig. 8a. Actually, the negative OLR anomaly on the periphery of Antarctica, referred to previously, centered at 120°W, is also correlated with the frontal activity over that region as well. It is interesting to note that the large negative frontal activity anomaly over the SEPz region is actually consistent with the positive anomaly of OLR over that region. This suggests very strongly that the production of the high pressure system over the SEP area inhibits frontal activity, inducing consistently less precipitation and probably large positive OLR anomalies.

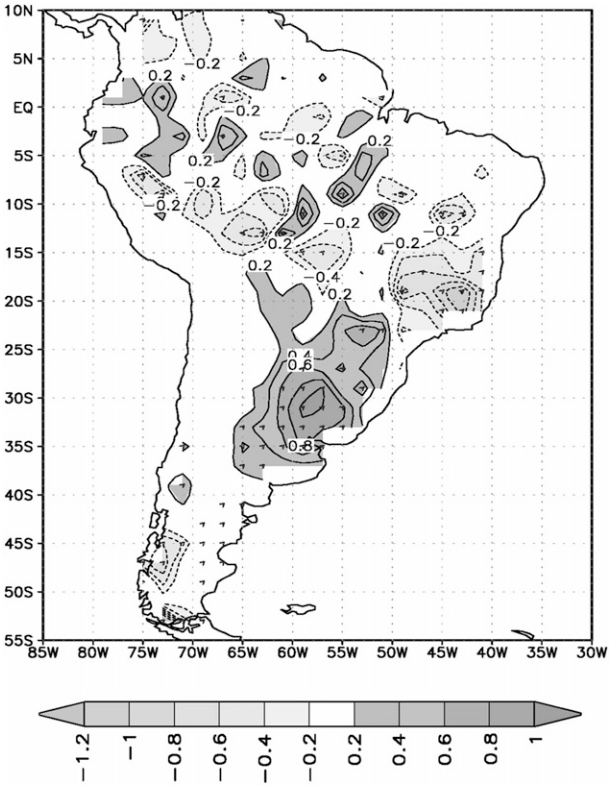

FIG. 7. Regression of the daily precipitation field with the SEPz time series, computed for OND of the period 1979–99. Contours are drawn every 0.2 mm day^{-1}, zero contours omitted. Light (dark) shading and dashed (solid) contours correspond to negative (positive) precipitation anomalies. Stippled areas indicate where the correlation is significant at the 95% confidence level.

Figure 8b also suggests that the frontal activity seems to pass through the south of the high, enters South America, and moves northeastward. Consequently, that high works as a common blocking event (Sinclair 1996; Renwick 2005). The influence of blocking events over the southeastern Pacific Ocean on transient systems affecting South America has been referred to by Mendes et al. (2008), who suggest a northward track of the synoptic systems related to the presence of blocking over the SEP.

To confirm that the precipitation pattern over LPB and SACZ is influenced by the frontal activity, we performed a lagged regression between the FI and the precipitation time series at the LPB and SACZ. Since the temporal scale of the precipitation related to frontal activity is rather small because it relates precipitation events with synoptic-scale processes, we have bandpass filtered the precipitation time series, retaining the periods between 2.5 and 14 days. Figure 9 shows the sequence of lagged regression for the LPB from two days prior to two days after the rainy event. This figure clearly shows that two days prior to the rainy event over LPB there is a maximum of frontal activity over southwestern South America. The frontal activity progresses to a large maximum over the LPB region at time lag 0 and two days later the large frontal activity is shifted toward the South Atlantic Ocean, explaining what we noted in Fig. 8b, where we found strong frontal activity located over subtropical South America extending over the South Atlantic Ocean. Precipitation over the SACZ also relates to frontal passages, but the intensity of the regression is much weaker compared with LPB (not shown). These transient systems propagate toward the northeast and only some of them reach lower latitudes, organizing convection over the SACZ (Siqueira and Machado 2004).

Overall, the relationship between frontal activity and rainfall over the LPB and SACZ is consistent with the results shown in Liebmann et al. (2004), who pointed out that the evolution of baroclinic systems affects rainfall over the subtropical plains and to a lesser extent over the SACZ, using a different approach.

It is clear that the frontal activity controls the high-frequency variability of precipitation over South America, mainly over the LPB region. However, the synoptic-scale activity is conditioned by the presence of the anomalous high over the southeastern South Pacific Ocean, which influences the trajectory of synoptic systems and consequently influences precipitation. How this quasi-stationary circulation anomaly is maintained is an issue that we will try to elucidate elsewhere.

4. Discussion on the time scales of variability of the circulation anomalies

To better understand the time scales involved in the SEPz time series we calculated the variance of the bandpass-filtered anomalies of the 500-hPa geopotential for the Southern Hemisphere, corresponding to the large peaks of Fig. 5. We filtered the 500-hPa geopotential anomalies, retaining the periods from 35 to 60 days, 21 to 26 days, and 14 to 17 days, respectively, and computed the variance (shown in Fig. 10). It is interesting to point out that the maximum variance of the 500-hPa geopotential in all time scales is centered at the region where we defined the SEPz. For very low frequencies, a band of maximum variance extending from west of the Ross Sea to the end of the Weddell Sea area can be noted, with a secondary maximum located to the southwest of Australia, probably corresponding to blocking events that are frequent in that region (Sinclair 1996). On intermediate scales, corresponding to periods from 21 to 26 days, the spatial structure of the variance field also depicts three regions with maximum variance, located to the southwest of Australia, over the Ross Sea, and over the Weddell Sea, similar to

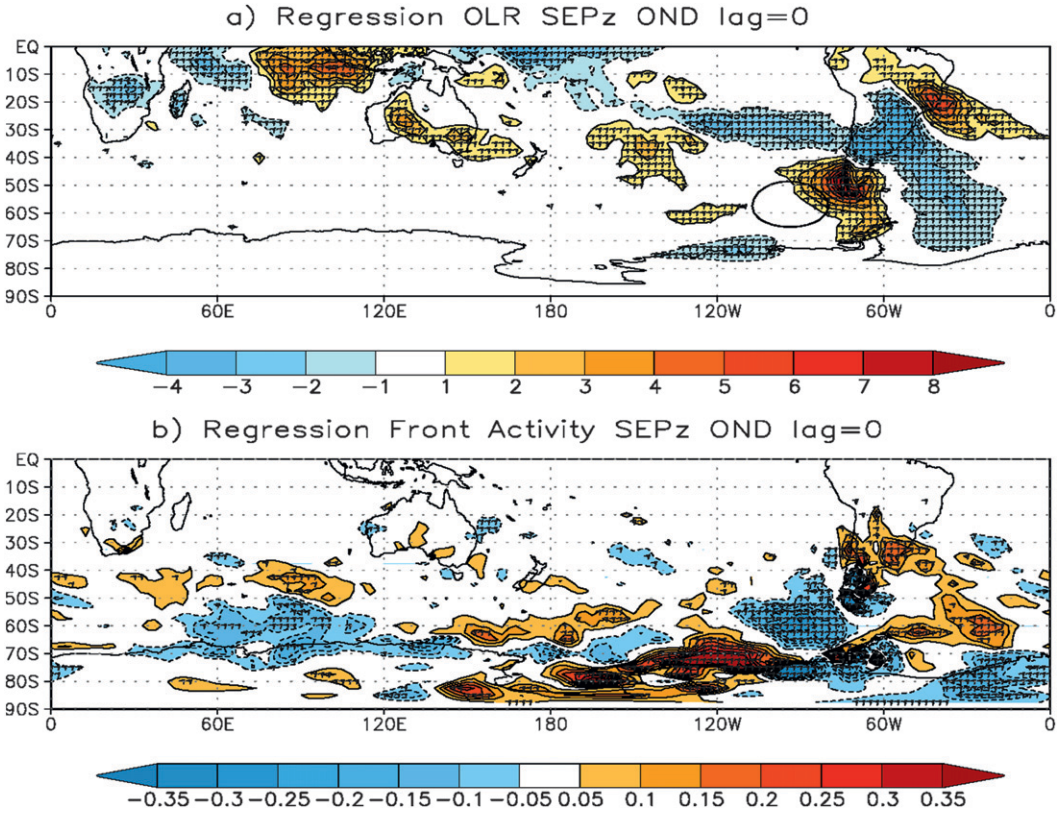

FIG. 8. (a) Regression of the daily OLR anomaly field with the SEPz time series. Contours are drawn every 1 W m^{-2}, zero contours omitted. Blue (orange) shading and dashed (solid) contours correspond to negative (positive) OLR anomalies. Stippled areas indicate where the correlation is significant at the 95% confidence level. The 1000 m^2 s^{-2} contour (heavy solid line) corresponding to the 500-hPa geopotential anomaly field regressed against the SEPz time series is drawn for reference. (b) As in (a) but for the FI. Contours are drawn every 0.05°C m^{-1} s^{-1}.

the variance corresponding to the lower frequencies. However, for higher frequencies, with periods from 14 to 17 days, the most remarkable feature is the large maximum over the SEP region, which is strongly related to storm tracks that contain most of these frequency bands. To verify this behavior we have taken a test function over southwestern Australia, averaging the 500-hPa height anomalies over a box centered at 50°S, 105°W, referred to as the SAU region (the box in Fig. 10a), and calculated the spectrum (shown in Fig. 5). The spectrum for the SAUz time series shows a main peak in the low frequencies and a secondary peak corresponding to periods from 21 to 26 days. The spectral amplitude at higher frequencies is definitely reduced, in agreement with Fig. 10.

The connection between the anomalous high over the SEP region and the rest of the variability of the circulation over the Pacific Ocean on intraseasonal time scales could have different origins. One could be tropical convection, which serves as a catalyst in the development of the PSA modes (Mo and Higgins 1998). The PSA modes attain the largest amplitudes in the Pacific–South American sector (Mo 2000, and references therein) and contain the quasi-stationary anomalous anticyclonic circulation over the southeastern Pacific Ocean. The other possibility is that the Indian Ocean dipole could also produce a similar PSA response (Chan et al. 2008). Moreover, owing to the robustness of this signal, OS10 have recently shown that there is a mutual interaction between a thermal forcing and an anomalous high more prevalent in the subpolar regions (a brief summary of OS10 can be found in the appendix). The reason is that, if there is a barotropic signal of an anomalous high that is produced by remote processes, that anomaly could organize convection by removing sea ice and fluxing moisture southward to the subpolar regions. The convection localized in the western part of the anomalous high, apparent in Fig. 8a as a positive OLR anomaly, can produce a thermal forcing that will enhance the anomalous high, producing a mutual interaction between convection and the high anomaly

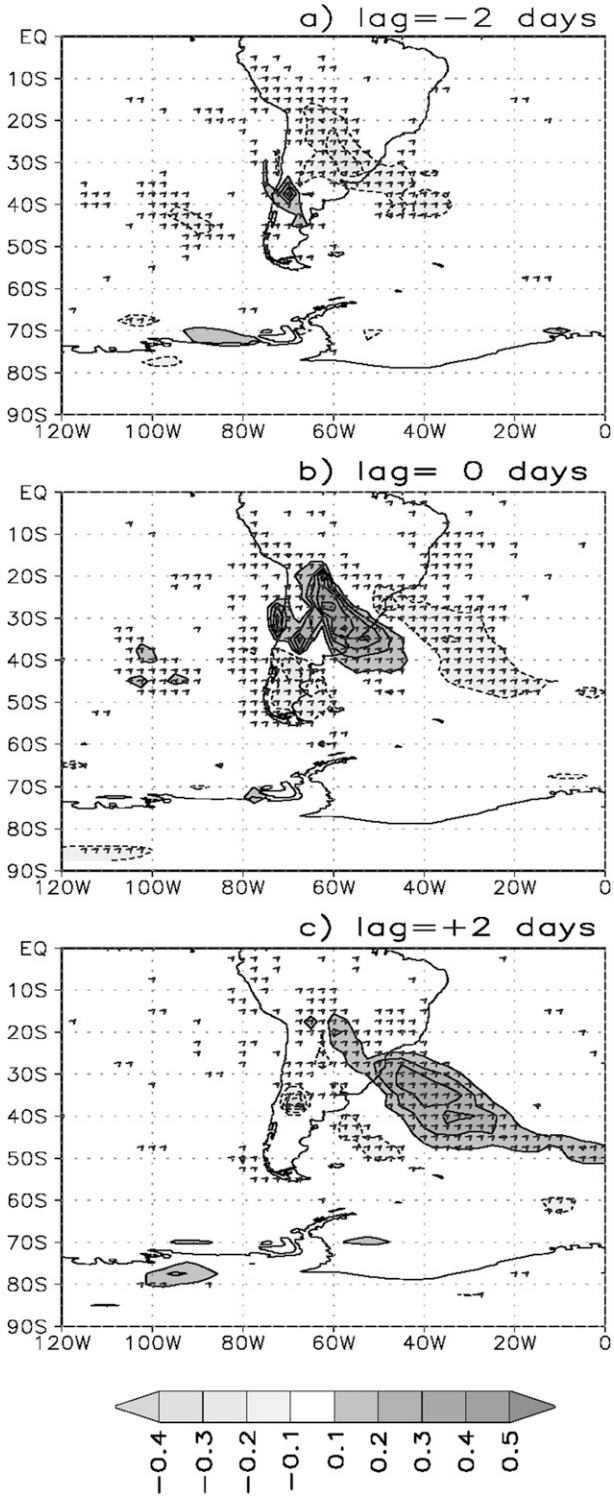

FIG. 9. Lagged regression of the daily field of Front Activity Index with the bandpass-filtered (2.5–14 days) precipitation time series for LPB for lag (a) −2, (b) 0, and (c) +2 days: contours every 0.1°C m^{-1} s^{-1}. Light (dark) shading and dashed (solid) lines correspond to negative (positive) values. Stippled areas indicate where the correlation is significant at the 95% confidence level.

itself. That convection tends to produce latent heating on the western side of the anomalous high that, in turn, can enhance the response of the high anomaly. Consequently, the anomalous high over the southeastern Pacific Ocean may be supported by a positive feedback mechanism. The diabatic forcing in the southeastern Pacific Ocean may also trigger external Rossby waves that couple with the Rossby waves excited remotely, reinforcing the anomalous circulation toward South America. To clarify to what extent the anomalous high over the southeastern South Pacific is responsible for exciting Rossby waves that propagate toward the northeast over South America, we have included an appendix with results obtained with an idealized model. These results are analyzed in depth in OS10.

5. Summary and conclusions

The focus of the research presented here is to explore the mechanisms explaining the intraseasonal variability of rainfall over South America during the austral spring season, characterized by a dipole pattern, with centers of action located over the SACZ and LPB. We center our attention on the spring season because it is the onset of the rainy season in South America and also because we are more interested on exploring the mechanisms triggering precipitation variability over LPB, which has an annual cycle characterized by maximum rainfall during late summer to early fall (February and April) and late spring (November).

The spectral analysis of the time series of precipitation and OLR anomalies built for SACZ and LPB revealed robust peaks at intraseasonal and synoptic time scales, in agreement with Liebmann et al. (1999). The intensity of spectral maxima for lower frequencies is larger for the SACZ compared with the LPB and the opposite occurs for higher frequencies.

We have analyzed the circulation anomalies associated with precipitation over South America by performing a time-lagged regression analysis of the 500-hPa geopotential height anomaly field with the time series of precipitation anomalies over the SACZ and LPB. Results for the LPB showed that the most prominent feature is the presence of a quasi-stationary anomalous high over the southeastern South Pacific Ocean and, emanating from that high, a trend of ''external'' Rossby waves propagating toward South America. When LPB (SACZ) precipitation is anomalously large, this Rossby wave pattern exhibits a cyclonic (anticyclonic) circulation over central Argentina and an anticyclonic (cyclonic) circulation over southeastern Brazil, favoring moisture flux convergence toward the LPB (SACZ) region. This result was also found by previous studies (Liebmann et al. 1999; 2004;

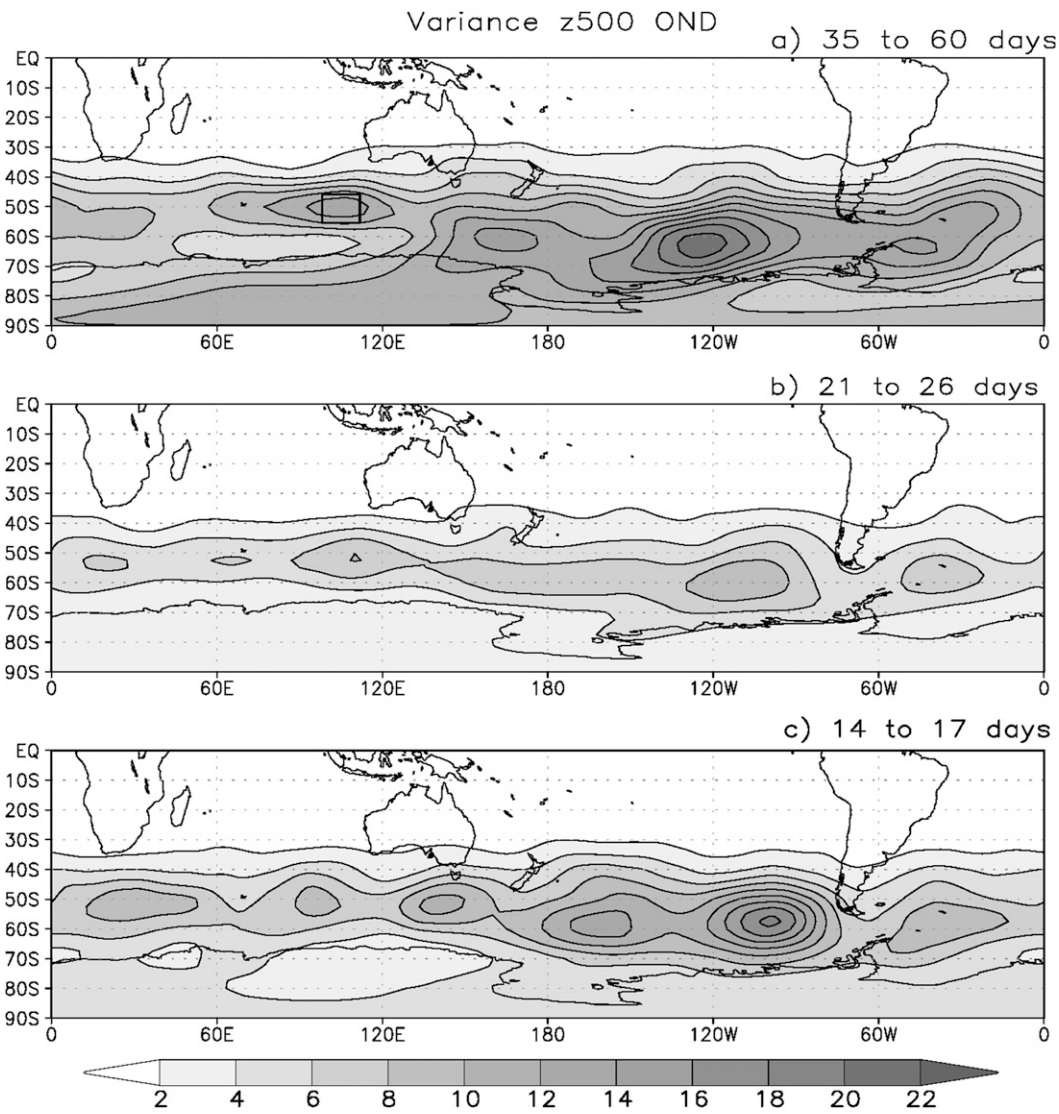

FIG. 10. Variance of the daily 500-hPa geopotential filtered anomalies retaining periods from (a) 35 to 60, (b) 21 to 26, and (c) 14 to 17 days. The variance has been divided by a factor of 10^4 for clarity. Contours are drawn every 2×10^4 m^4 s^{-4}. The box in (a) defines the SAU area where the anomalies of 500-hPa heights were averaged to define the SAUz time series.

Nogués-Paegle and Mo 1997; among others). These authors interpreted this behavior as the influence of a Rossby wave originating over the midlatitudes in the Pacific Ocean and suggested that the phase of the wave approaching South America determines whether rainfall will be enhanced over the SACZ or over the LPB. We have demonstrated that the presence of an anomalous high circulation located over the southeastern Pacific Ocean controls the behavior of Rossby wave trains propagating over South America (see appendix).

To explore the behavior of the quasi-stationary anomalous high, we defined an index, referred to as SEPz, averaging the geopotential height anomalies at 500 hPa over that region. The spectral analysis of this time series revealed that the time scales of variability of this quasi-stationary anomaly are compatible with the time scales of variability of precipitation over South America and also with the time scales of variability of one of the leading modes of intraseasonal variability of the atmospheric circulation in the Southern Hemisphere, the well-known PSA2 pattern.

Several previous studies have suggested that synoptic-scale activity generated within the South Pacific storm track may trigger severe storms in an unstable atmospheric

environment over both LPB and SACZ regions. Cunningham and Cavalcanti (2006) showed that the frontal systems sweeping over South America in the presence of the PSA-like pattern could trigger convection over the SACZ. We have demonstrated that the frontal systems are strongly related with precipitation over the LPB. Moreover, the preference for the frontal system path is controlled by the anomalous high over the SEP area. Therefore, the high-frequency activity is actually modulated by circulation variability at lower frequencies.

The connection between the anomalous high over the SEP region and the rest of the variability over the South Pacific Ocean could have different origins (the PSA or the Indian dipole, among others). However, the behavior of this quasi-stationary circulation anomaly may be supported by the interaction with surface conditions by a positive feedback mechanism. OS10 have recently shown that there is a mutual interaction between a thermal forcing and an anomalous high more prevalent in the subpolar regions. Once a barotropic signal of an anticyclonic anomaly is produced by remote processes, this anomalous high induces warm advection over its western side, which may reduce the sea ice extent. When warm air blows over a colder surface, it produces a wedge forcing the warm air to rise. This forced convection induces the production of diabatic heating from latent heat release, which in turns reinforces the anomalous high. This process of mutual interaction could explain the persistent large amplitude of the external Rossby waves in the Pacific–South American sector. In a future work we will explore more on the variability of this high on longer time scales in relation to the lower frequency variability of rainfall over South America.

Acknowledgments. We thank Thomas Knutson for reviewing the manuscript and suggesting insightful comments. We wish to thank B. Liebmann and two anonymous reviewers for useful discussions and comments that have certainly led to improvements in the manuscript. This work has been supported by ANPCyT Grant PICT2005 32194 and UBACyT Grant X160 and by the Argentinean Raices Programme of the University of Buenos Aires. Particular thanks are due to Dr. C. Vera for making possible Dr. Isidoro Orlanski's visit to CIMA. One of the authors, Isidoro Orlanski, was supported by Grants NA17RJ2612 and NA08OAR4320752 from the National Oceanic and Atmospheric Administration, U.S. Department of Commerce. The statements, findings, conclusions, and recommendations are those of the author(s) and do not necessarily reflect the views of the National Oceanic and Atmospheric Administration or the U.S. Department of Commerce.

APPENDIX

External Rossby Waves as a Response to Sources of Vorticity and Thermal Forcing[1]

In the following section, we will demonstrate that the diabatic heating due to, for example, convection organized by a stationary wave could effectively destabilize these waves. We will present an abbreviated review of results from a spectral global atmospheric model forced with idealized local thermal and vorticity sources. It was demonstrated earlier (OS10) that, if the diabatic heating occurs in a particular section of the external wave, this heating could enhance the wave itself.

The discussion in previous sections shows that a positive height anomaly over the southeastern Pacific Ocean occurs very frequently and that there are different mechanisms that generate a similar response. The interpretation seems straightforward: a high pressure system located over subpolar regions produces advection of heat and moisture due to the poleward wind blowing warm, moist air into the frigid zone of the Antarctic coast. Moreover, it has been shown that an isolated thermal heating will force a high on the downstream side (Hoskins and Karoly 1981; Held 1983; Held and Ting 1990; among others). Therefore, under some conditions, the diabatic heating produced by the warm advection on the western side of a high pressure system could, indeed, produce a feedback to maintain that high. This is the central hypothesis of OS10. It should be pointed out that—as described by Hoskins and Karoly (1981) and Held (1983)—the single thermal forcing tends to produce a low-level low pressure center with equatorward flow over the thermal forcing such that the heat advection balances the diabatic heating. Of course, this circulation would be against the possibility of advecting moisture to the thermal forcing; consequently, it could not be an efficient mutual interaction between the external wave and the thermal forcing as it is postulated. However, we will show that the low-level circulation could be reversed by adding an equivalent barotropic external wave that has been remotely generated, as in the case of Rossby waves that propagate from the subtropics to high latitudes—for example, those excited by a source of diabatic heating over the tropical Pacific Ocean during El Niño events. Although a large number of studies focus on the forcing of the external Rossby waves by a thermal source, little has been done to explore the possibility of mutual interaction of a Rossby wave and the thermal source as in OS10.

[1] This is a summary of some runs presented in Orlanski and Solman (2010).

The spectral model described in Held and Suarez (1994)[2] was used to compare benchmark simulations so as to evaluate different atmospheric general circulation models independently of physical parameterizations. The model is a standard hydrostatic, *s*-coordinate, semi-implicit, spectral transform model in vorticity–divergence prognostic equations. The vertical differencing uses the simplest centered differences, and the hydrostatic equation is integrated analytically assuming that temperature is constant within each layer. There are 20 vertical levels, equally spaced in sigma, with the top of the model formally set to a zero pressure. The horizontal mixing of vorticity, divergence, and temperature takes the form of a Laplacian raised to the fourth power, with the strength set so that the *e*-folding time for the smallest wave in the system is always 0.1 days. The truncation is triangular. All integrations shown are for T63 resolution.

Results from a series of runs that were made to evaluate the external Rossby wave response to diabatic forcing for a shallow surface heating are presented. Also, solutions with a localized vorticity source alone and in combination with the thermal source are discussed. The global model was initialized with a mean solution for an idealized aquaplanet, as in Held and Suarez (1994). Three solutions were run, one with a vorticity forcing center at 60°S (control), one in which thermal and vorticity forcing were included in the high latitudes (60°S), and finally one solution in which the vorticity forcing was as for the control and a thermal forcing center at 28°S to simulate the convection over LPB.

The localized thermal forcing has the form

$$\frac{\partial}{\partial t}T = \ldots\, k_T(\varphi, \sigma)[T - T_{\mathrm{eq}}(\varphi, p)] + \frac{\partial}{\partial t}F,$$

$$\frac{\partial}{\partial t}F = (\Delta\theta)_t \exp\left[-\left(\frac{x - x_0}{x_{\mathrm{wid}}}\right)^2\right] \exp\left[-\left(\frac{y - y_0}{y_{\mathrm{wid}}}\right)^2\right] \times 0.5\left[1. + \tanh\left(\frac{P - \delta P_0}{P_{\mathrm{th}}}\right)\right], \quad \text{(A1)}$$

where dF/dt represents the diabatic forcing, usually in cases of shallow, high-latitude heating. The amplitude is $(\theta)_t$ (assumed to be ~2 K day^{-1}), and x_0 and y_0 are the center of the forcing, with a decay in the zonal direction x_{wid} and latitudinal direction of y_{wid}. The vertical distribution is maximum at the ground, with a decay with a thickness P_{th} centered at δP_0.

The vorticity source defined below is introduced in the equations as a local height anomaly tendency that geostrophically corresponds to a vorticity forcing. The shape of the local forcing is similar to the heat source [Eq. (A1)] but maximized at the upper level with a vertical structure such that $\delta P_0 = 600$ hPa:

$$\frac{\partial}{\partial t}F_{h\mathrm{vort}} = h\mathrm{vort}_0 \exp\left[-\left(\frac{x - x_0}{x_{\mathrm{wid}}}\right)^2\right] \exp\left[-\left(\frac{y - y_0}{y_{\mathrm{wid}}}\right)^2\right] \times 0.5\left[1.0 - \tanh\left(\frac{P - \delta P_0}{P_{\mathrm{th}}}\right)\right],$$

$$\frac{\partial}{\partial t}\mathbf{v} + \ldots = -\mathbf{k}x\frac{\partial}{\partial t}\nabla F_{h\mathrm{vort}}. \quad \text{(A2)}$$

The vorticity forcing was applied to the zonal and meridional momentum equations [Eq. (A2)]. Since the purpose of this work is to show a possible interaction between an external wave far remotely generated and the localized thermal forcing, we simplified the forcing of the upper-level vorticity to generate an equivalent barotropic response similar to that generated remotely. In Fig. A1 the three responses are shown; the upper graph shows the response to only upper-level vorticity forcing, which as expected produces a high over the forcing and a train of external Rossby waves that emanate from the high to lower latitudes, in agreement with Berbery et al. (1992). The middle graph of Fig. A1 shows the response when a lower-level thermal forcing was added to the upper-level vorticity forcing: the response is similar to the previous one, but with a larger amplitude of the high over the eastern part of the thermal forcing. The upper-level vorticity forcing produced a barotropic response as expected, whereas the diabatic heating tends to produce a more tilted response, as discussed previously (Hoskins and Karoly 1981; Held 1983). The combination of both forcings could be more or less barotropic, depending on the strength of both forcings. This case with the two forcings located at 60°S was done to stress the results of the enhancement of the high anomaly over the southeastern Pacific Ocean, as discussed in OS10. The upper-level forcing was positioned such that the external wave generated by the vorticity forcing is approximately in quadrature with the thermal forcing. This allows poleward flow over the thermal forcing region and, as was shown in OS10, permits moisture fluxes over the thermal forcing region. It should be pointed out that not only the enhancement occurs when an external wave propagates to the high latitudes, but it increases the possibility of organizing convection, as in the previous case.

Furthermore, a geopotential high forced at high latitudes produces a train of external waves that propagates northeastward to the low latitudes; if convection is possible, it will enhance the local response over the thermal

[2] The code for this model is available upon request (from isaac.held@noaa.gov).

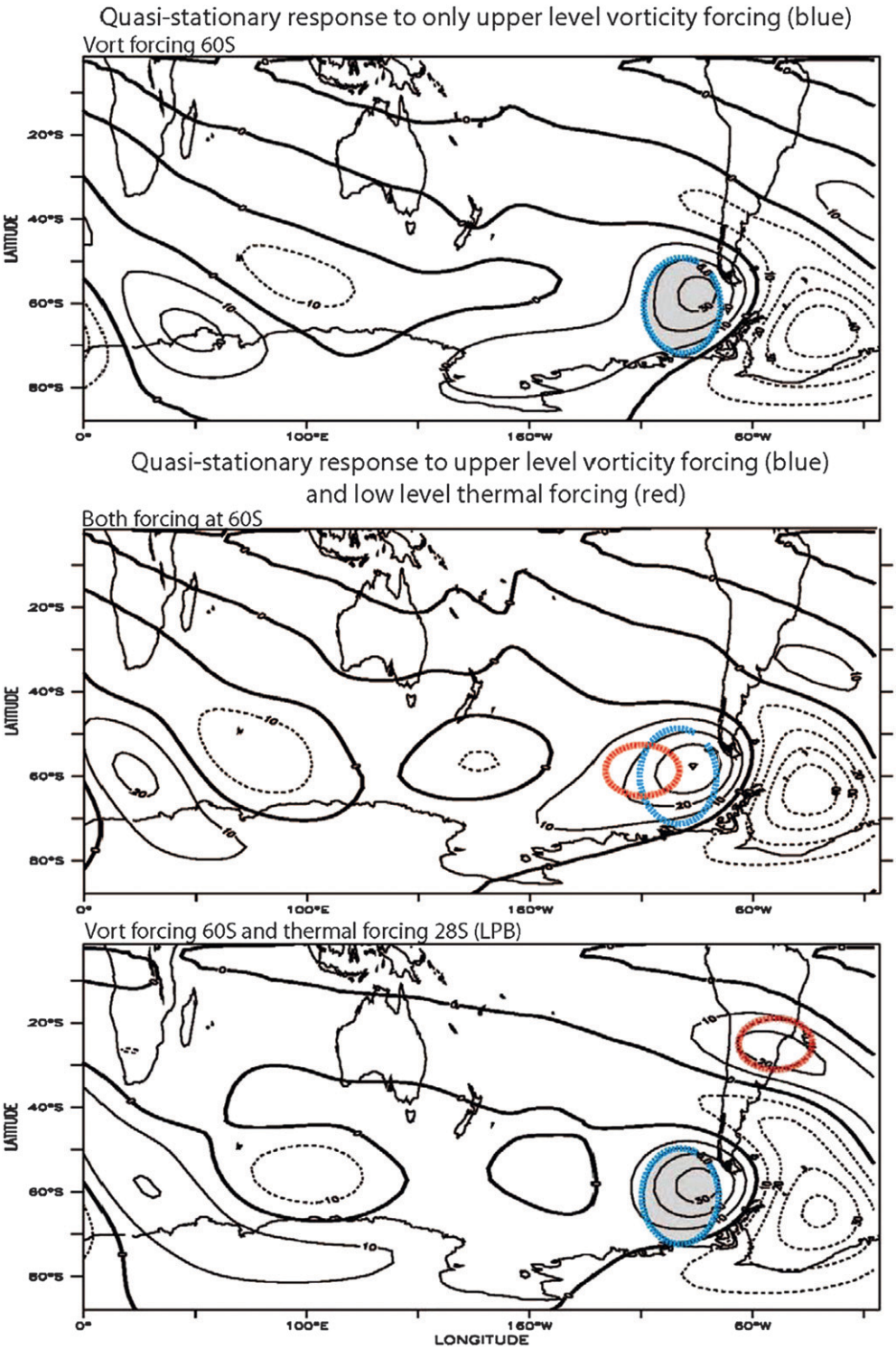

FIG. A1. Long-time-averaged (1000 day) 300-hPa height anomaly of the quasi-stationary response to vorticity and thermal forcing for (top) only vorticity forcing (blue contour) and height response (contour 10 m); (middle) combined vorticity (blue contour) and thermal (red contour) forcing; and (bottom) combined response for subpolar vorticity forcing and subtropical thermal forcing, simulating the convection over the LPB. The geography is only shown for reference; none of the simulations has land or topography. Thermal forcing contour (red) is 0.25 K day^{-1} and vorticity forcing (height forcing) 5 m day^{-1}.

forcing as well. This is shown in the lower graph of Fig. A1. The upper-level vorticity forcing was located as in Fig. A1a but it also included a thermal forcing close to where the external high collocates in the subtropics (around the LPB region ~28°S). No effort has been made for these simulations to reproduce the signal of the regression results shown in previous sections. The spectral model did not include topography or moisture, and the mean flow is, as mentioned above, a climatological idealization discussed in Held and Suarez (1994). Actually, the result points to the fact that one does not need topography to simulate the external wave response.

REFERENCES

Ambrizzi, T., and B. J. Hoskins, 1997: Stationary Rossby-wave propagation in a baroclinic atmosphere. *Quart. J. Roy. Meteor. Soc.,* **123,** 919–928.

Berbery, E. H., J. Nogués-Paegle, and J. Horel, 1992: Wavelike Southern Hemisphere extratropical teleconnections. *J. Atmos. Sci.,* **49,** 155–177.

Bloomfield, P., 1976: *Fourier Analysis of Time Series: An Introduction*. Wiley, 261 pp.

Carvalho, L. M. V., C. Jones, and B. Liebmann, 2004: The South Atlantic convergence zone: Intensity, form, persistence, and relationships with intraseasonal to interannual activity and extreme rainfall. *J. Climate,* **17,** 88–108.

Chan, S. C., S. K. Behera, and T. Yamagata, 2008: Indian Ocean dipole influence on South American rainfall. *Geophys. Res. Lett.,* **35,** L14S12, doi:10.1029/2008GL034204.

Cunningham, C., and I. Cavalcanti, 2006: Intraseasonal modes of variability affecting the South Atlantic convergence zone. *Int. J. Climatol.,* **26,** 1165–1180.

Díaz, A., and P. Aceituno, 2003: Atmospheric circulation anomalies during episodes of enhanced and reduced convective cloudiness over Uruguay. *J. Climate,* **16,** 3171–3185.

Duchon, C. E., 1979: Lanczos filtering in one and two dimensions. *J. Appl. Meteor.,* **18,** 1016–1022.

Garreaud, R. D., and J. M. Wallace, 1998: Summertime incursions of midlatitude air into subtropical and tropical South America. *Mon. Wea. Rev.,* **126,** 2713–2733.

Ghil, M., and K. C. Mo, 1991: Intraseasonal oscillations in the global atmosphere. Part II: Southern Hemisphere. *J. Atmos. Sci.,* **48,** 780–790.

Grimm, A. M., and P. L. Silva Dias, 1995: Analysis of tropical–extratropical interactions with influence functions of a barotropic model. *J. Atmos. Sci.,* **52,** 3538–3555.

Held, I. M., 1983: Theory of stationary eddies. *Large-Scale Dynamical Processes in the Atmosphere,* B. Hoskins and R. Pearce, Eds., Academic Press, 127–168.

——, and M. Ting, 1990: Orographic versus thermal forcing of stationary waves: The importance of the mean low-level wind. *J. Atmos. Sci.,* **47,** 495–500.

——, and M. Suarez, 1994: A proposal for the intercomparison of the dynamical cores of atmospheric general circulation models. *Bull. Amer. Meteor. Soc.,* **75,** 1825–1830.

Hoskins, B. J., and D. J. Karoly, 1981: The steady linear response of a spherical atmosphere to thermal and orographic forcing. *J. Atmos. Sci.,* **38,** 1179–1196.

——, and K. I. Hodges, 2005: A new perspective on Southern Hemisphere storm tracks. *J. Climate,* **18,** 4108–4129.

Kalnay, E., and Coauthors, 1996: The NCEP/NCAR 40-Year Reanalysis Project. *Bull. Amer. Meteor. Soc.,* **77,** 437–471.

Kayano, M., 1999: Southeastern Pacific blocking episodes and their effects on the South American weather. *Meteor. Atmos. Phys.,* **69,** 145–155.

Liebmann, B., and C. A. Smith, 1996: Description of a complete (interpolated) outgoing longwave radiation dataset. *Bull. Amer. Meteor. Soc.,* **77,** 1275–1277.

——, G. N. Kiladis, J. A. Marengo, T. Ambrizzi, and J. D. Glick, 1999: Submonthly convective variability over South America and the South Atlantic convergence zone. *J. Climate,* **12,** 1877–1891.

——, ——, C. Vera, A. C. Saulo, and L. M. V. Carvalho, 2004: Subseasonal variations of rainfall in South America in the vicinity of the low-level jet east of the Andes and comparison to those in the South Atlantic convergence zone. *J. Climate,* **17,** 3829–3842.

Mendes, M. C. M. D., R. M. Trigo, I. F. A. Cavalcanti, and C. C. DaCamara, 2008: Blocking episodes in the Southern Hemisphere: Impact on the climate of adjacent continental areas. *Pure Appl. Geophys.,* **165,** 1941–1962.

Mo, K., 2000: Relationships between low-frequency variability in the Southern Hemisphere and sea surface temperature anomalies. *J. Climate,* **13,** 3599–3610.

Mo, K. C., and R. W. Higgins, 1998: The Pacific–South American modes and tropical convection during the Southern Hemisphere winter. *Mon. Wea. Rev.,* **126,** 1581–1596.

Nijssen, B., R. Schnur, and D. P. Lettenmaier, 2001: Global retrospective estimation of soil moisture using the variable infiltration capacity land surface model, 1980–93. *J. Climate,* **14,** 1790–1808.

Nogués-Paegle, J., and K. C. Mo, 1997: Alternating wet and dry conditions over South America during summer. *Mon. Wea. Rev.,* **125,** 279–291.

——, L. A. Byerlee, and K. C. Mo, 2000: Intraseasonal modulation of South American summer precipitation. *Mon. Wea. Rev.,* **128,** 837–850.

Orlanski, I., and S. Solman, 2010: The mutual interaction between external Rossby waves and thermal forcing: The subpolar regions. *J. Atmos. Sci.,* in press.

Renwick, J. A., 2005: Persistent positive anomalies in the Southern Hemisphere circulation. *Mon. Wea. Rev.,* **133,** 977–988.

Salio, P., M. Nicolini, and E. Zipser, 2007: Mesoscale convective systems over southeastern South America and their relationship with the South American low-level jet. *Mon. Wea. Rev.,* **135,** 1290–1309.

Sinclair, M. R., 1996: A climatology of anticyclones and blocking for the Southern Hemisphere. *Mon. Wea. Rev.,* **124,** 245–263.

Siqueira, J. R., and L. U. T. Machado, 2004: Influence of the frontal systems on the day-to-day convection variability over South America. *J. Climate,* **17,** 1754–1766.

Velasco, I., and J. M. Fritsch, 1987: Mesoscale convective complexes in the Americas. *J. Geophys. Res.,* **92** (D8), 9591–9613.

Vera, C., P. K. Vigliarolo, and E. H. Berbery, 2002: Cold season synoptic-scale waves over subtropical South America. *Mon. Wea. Rev.,* **130,** 684–699.

Wilks, D., 1995: *Statistical Methods in the Atmospheric Sciences: An Introduction*. Academic Press, 467 pp.